Journal of Statistical Physics, Vol. 86, Nos. 1/2, 1997

Error Estimates for the Fast Multipole Method

Dorthe Sølvason[1] and Henrik G. Petersen[1]

Received December 4, 1995; final April 1, 1996

Error estimates for algorithms based on truncations for evaluating electrostatic interactions in molecular dynamics applications are very important for several reasons. For example, the estimates are necessary to establish the validity of the simulations and can be used to estimate various simulation parameters. Very precise estimates have been found for the Ewald method and the related particle mesh Ewald method. However, for the very popular fast multipole method such a precise estimate is not available. In this paper, we illustrate the rather complicated error behavior of the fast multipole method and we use statistical methods to derive an estimate for the root mean square error on the forces. Furthermore, the expected maximum error on the force acting on a single particle is studied. The estimates are tested against errors obtained from simulations and are found to be very precise.

KEY WORDS: Electrostatic pair interactions; fast multipole method; estimates of errors due to truncations.

1. INTRODUCTION

With the increase of computer power, molecular dynamics simulations of large systems containing proteins, polymers, and solvent molecules have become an important method for understanding various mechanisms in, for example, the human body. However, if such simulations are to be relied on, the forces on the atoms must be calculated precisely. There are two types of nonbonded pair forces which act on atoms in classical mechanical pictures of condensed matter

- Short-ranged (van der Waals) forces
- Electrostatic forces

[1] Center for Mathematical Modelling and Numerical Simulation Department of Information Technology, Odense University, DK-5230 Odense M, Denmark.

822/86/1-2-26

Modern molecular dynamics simulations use very large samples. To bring down computation time within reasonable bounds, the forces cannot be calculated exactly, they are rather approximated to some specific accuracy. It is very important to understand what the error on the force is as a function of the approximation. The short-ranged forces are approximated by simply neglecting interactions at distances bigger than some cutoff. The error behavior as a function of the cutoff is well understood[2].

In this paper we shall study the error in the long-ranged electrostatic interactions when calculated using the fast multipole method. The error behavior of these interaction approximations is much more complicated than for the error in using a cutoff for the short-ranged interactions.

The model system that we are going to study consists of N charges $q_1,..., q_N$ (satisfying $\sum_{j=1}^{N} q_j = 0$) positioned at $\mathbf{R}_1,..., \mathbf{R}_N$ in a cubic box (of sidelength Λ). The box is embedded in a three-dimensional infinite array of copies of the box. The overall potential energy of the N charges can then be written as

$$U_s(\mathbf{r}_1,..., \mathbf{r}_N) = \frac{1}{2\Lambda} \lim_{K \to \infty} \sum_{\substack{\mathbf{n} \in \mathbb{Z}^3 \\ |\mathbf{n}| < K}}^{*} \sum_{i=1}^{N} \sum_{j=1}^{N} \frac{q_i q_j}{|\mathbf{r}_i - \mathbf{r}_j + \mathbf{n}|} \tag{1}$$

where $\mathbf{r}_i = \mathbf{R}_i/\Lambda$, $i = 1,..., N$, and where the asterisk indicates that the terms $i = j$, $\mathbf{n} = \mathbf{0}$ are to be omitted. Notice that we have assumed the summation order to be spherical. Other shapes of summation lead to different values.[4] However, the results of this paper can easily be generalized to those cases. Below we shall assume that the spherical array of copies is surrounded by a conductor (truly periodic boundary conditions).

Whatever method is used to calculate the electrostatic forces, truncations have to be made which lead to errors in the potential energy and in the forces on the charges. A very significant, widely used, and robust error measure is

$$\delta f_{\text{rms}} = \left[\frac{1}{N} \sum_{i=1}^{N} (\mathbf{f}_i^{\text{exact}} - \mathbf{f}_i^{\text{approx}})^2 \right]^{1/2} \tag{2}$$

where $\mathbf{f}_i^{\text{exact}}$ is the exact force acting on charge number i and $\mathbf{f}_i^{\text{approx}}$ is the force acting on the ith charge when calculated by some approximate method. Also of interest is the maximum error on the force on a single particle,

$$\delta f_{\max} = \max_{i=1,..., N} [(\mathbf{f}_i^{\text{exact}} - \mathbf{f}_i^{\text{approx}})^2]^{1/2} \tag{3}$$

In order to get relative error measures, we use the exact root mean square force

$$f_{\text{rms}} = \left[\frac{1}{N} \sum_{i=1}^{N} (\mathbf{f}_i^{\text{exact}})^2 \right]^{1/2} \tag{4}$$

and we can thus define the relative root mean square error on the force

$$\varepsilon_{\text{rms}} = \delta f_{\text{rms}} / f_{\text{rms}} \tag{5}$$

and the relative maximum error on the force

$$\varepsilon_{\max} = \delta f_{\max} / f_{\text{rms}} \tag{6}$$

The form of the potential U_s in Eq. (1) corresponds to a pair interaction potential which is not periodic if the dipole moment of the basic cube is not zero. The potential U for the truly periodic case differs from U_s by a term proportional to the square of the dipole moment of the cube.[4] This potential U can be rewritten in several much more computationally useful forms, which we now review.

One way is the famous Ewald method,[4] where the truly periodic potential energy can be written as

$$\begin{aligned} U(\mathbf{r}_1, \ldots, \mathbf{r}_N) = \frac{1}{A} \Bigg[& \sum_{\mathbf{n} \in \mathbb{Z}^3} \sum_{1 \leqslant i < j \leqslant N} \frac{\operatorname{erfc}(\alpha |\mathbf{r}_i - \mathbf{r}_j + \mathbf{n}|)}{|\mathbf{r}_i - \mathbf{r}_j + \mathbf{n}|} \\ & + \sum_{\substack{\mathbf{k} \in \mathbb{Z}^3 \\ \mathbf{k} \neq \mathbf{0}}} \frac{\exp(-\pi^2 \mathbf{k}^2 / \alpha^2)}{2\pi \mathbf{k}^2} \sum_{j=1}^{N} \sum_{l=1}^{N} q_j q_l \exp[2\pi i \mathbf{k} \cdot (\mathbf{r}_j - \mathbf{r}_l)] \\ & - \frac{\alpha}{\sqrt{\pi}} \left(\sum_{j=1}^{N} q_j^2 \right)^{1/2} \Bigg] \end{aligned} \tag{7}$$

When using the Ewald method for computing the potential energy and the corresponding forces, only the minimum image term is included for each pair $\{i, j\}$ of charges in the first term of (7). That is, instead of using a sum over all $\mathbf{n} \in \mathbb{Z}^3$, only the term corresponding to $\mathbf{n}_{i,j} = \min_{\mathbf{n} \in \mathbb{Z}^3} |\mathbf{r}_i - \mathbf{r}_j + \mathbf{n}|$ is considered for each pair $\{i, j\}$. In practice the $\mathbf{k}$-sum is truncated at some $|\mathbf{k}| = K_{\max}$ and the $\operatorname{erfc}(x)$ sum is truncated at some cutoff $x = r_c$. The parameter α can be chosen arbitrarily.

For the Ewald method very precise theoretical estimates of δf_{rms} as a function of the truncation parameters r_c and $K_{\max}$ and the split parameter α have been found.[10] It has furthermore been shown that the ratio

$$\delta f_{\max} / \delta f_{\text{rms}} \tag{8}$$

stays close to the expected values for a Gaussian distribution (2.5–3.5 for $N = 10{,}000$–$1{,}000{,}000$). Similar results have been found for the particle mesh Ewald method.[3, 12] There are several advantages of having such estimates: For a given value of α and desired accuracy, the truncation parameters r_c and $K_{\max}$ can be predicted theoretically by inverting the estimates. An optimization procedure may then be applied to choose the α value that minimizes the overall computation time. Apart from enabling an optimal parameter choice, the estimates provides a lot of insight into the method.

A very interesting and widely studied and applied method is the fast multipole method (FMM).[7] The FMM has an even more complicated parameter choice than the Ewald method and no successful prediction of a root mean square (rms) force error or any other average error measure has been accomplished. In this paper we study the rms force error as function of the chosen parameters. The error behavior turns out to be very complicated, but we have nonetheless found a very precise theoretical model for it. The precision is illustrated by comparisons with experimental results. A particular observation is that the ratio $\delta f_{\max}/\delta f_{\text{rms}}$ has huge non-Gaussian values. This estimate might be used to optimize computation time with respect to parameters in a way very similar to that used for the Ewald method, thus also providing new insight into the method. We shall discuss this briefly in the conclusion. The paper is organized as follows: In Section 2 we provide a description of the FMM. Section 3 is the main section and contains the derivation of the error estimates. The results are summarized in Section 4 and compared to experimental results in Section 5. We conclude the paper by some remarks about the qualitative error behavior and perspectives arising from the estimates found.

2. THE FAST MULTIPOLE METHOD (FMM)

In this section we will give a short description of the FMM, making it clear how it works, but without going into all details. It contains several modifications to the standard description, in particular in the definition of the spherical harmonics used and the treatment of periodic boundary conditions.

Considering the potential acting on one charge, the idea applied in the FMM is to approximate the potential from distant charges by expansions and evaluate the contributions from nearby charges directly by pair interactions. The FMM uses external and internal expansions to approximate the electrostatic potential. The "external" and "internal" expansions are almost always called "multipole" and "local" expansions, respectively.

We shall therefore adopt these names. A multipole expansion is an infinite series of the form

$$\phi(\mathbf{r}) = \sum_{l=0}^{\infty} \sum_{m=-l}^{l} A_l^m \frac{Y_l^m(\hat{\mathbf{r}})}{r^{l+1}} \tag{9}$$

where $\mathbf{r} = (r, \theta, \phi)$ using spherical coordinates, and it describes the potential due to charges located in a sphere centered at the origin and it is valid outside the sphere. The coefficients A_l^m depend on the positions of the charges and are given in Appendix A. The functions Y_l^m are spherical harmonics (see below). Besides the creation of a multipole expansion, the operations on the expansions that will be used in the FMM are as follows, the translation of the center of a multipole expansion, the conversion of a multipole expansion into a local expansion, and the translation of the center of a local expansion. A local expansion can be written as

$$\phi(\mathbf{r}) = \sum_{l=0}^{\infty} \sum_{m=-l}^{l} B_l^m Y_l^m(\hat{\mathbf{r}}) r^l \tag{10}$$

and describes the potential due to charges located outside a sphere centered at the origin and is valid inside the sphere. The FMM uses the important observation that the sum of contributions from several multipole expansions, which are all valid in the domain of a local expansion, can be calculated by simply adding up contributions to the B_l^m from the individual expansions. In Appendix A, we give formulas for the B_l^m contributions as functions of the coefficients and expansion point of a given multipole expansion valid inside the sphere. In the FMM it is also necessary to translate multipole expansions and local expansions from one expansion point to another. Formulas for these are also listed in Appendix A.

Of course these expansions are all truncated, so they consist of a finite number of terms. We write the truncated expansions as

$$\phi_L(\mathbf{r}) = \sum_{l=0}^{L} \sum_{m=-l}^{l} A_l^m \frac{Y_l^m(\hat{\mathbf{r}})}{r^{l+1}}, \qquad \phi_L(\mathbf{r}) = \sum_{l=0}^{L} \sum_{m=-l}^{l} B_l^m Y_l^m(\hat{\mathbf{r}}) r^l \tag{11}$$

Using spherical coordinates and writing $\mathbf{r} = (r, \theta, \phi)$, we use one of the standard definitions of spherical harmonics:

$$Y_l^m(\hat{\mathbf{r}}) = \left[\frac{2l+1}{4\pi} \frac{(l-m)!}{(l+m)!}\right]^{1/2} P_l^m(\cos\theta) e^{im\phi} \qquad \text{for} \quad l \geqslant 0, \quad -l \leqslant m \leqslant l \tag{12}$$

where the associated Legendre polynomials are defined as

$$P_l^m(z) = (-1)^m (1-z^2)^{m/2} \frac{d^m}{dz^m} P_l(z) \qquad \text{for} \quad l \geqslant 0, \quad 0 \leqslant m \leqslant l \tag{13}$$

and

$$P_l^{-m}(z) = (-1)^m \frac{(l-m)!}{(l+m)!} P_l^m(z) \qquad \text{for} \quad l \geqslant 0, \quad 0 \leqslant m \leqslant l \tag{14}$$

where

$$P_l(z) = \frac{1}{2^l l!} \frac{d^l}{dz^l} (z^2-1)^l \qquad \text{for} \quad l \geqslant 0, \quad -1 \leqslant z \leqslant 1$$

Notice that our definition of the spherical harmonics is a little different from the one used by Greengard and Rokhlin.[8] Using the definition above (where the spherical harmonics are orthonormal), the theorems stating how to translate the center of a multipole expansion, convert a multipole expansion into a local expansion, and translate the center of a local expansion become a little simpler than the ones used by Greengard and Rokhlin (and others[9,5]). Furthermore, various results for spherical harmonics found in the literature may be applied directly.[6] We state our version of the theorems in Appendix A.

The FMM belongs to the class of tree algorithms, where the computational cell is repeatedly refined into smaller cells. Here the computational cell (which is a unit cube) is called refinement level 0. It is refined into eight equally sized cells, where each cell again is refined into eight even smaller cells and so on until some maximum refinement level S containing 8^S cells is reached.

In the FMM the term *nearest neighbors* or just *neighbors* is used. The nearest neighbors of a given cell at some refinement level are the cells which share a face, an edge, or a corner with the cell. Each cell has 26 nearest neighbors.

Another set of cells defined for all cells is the *interaction list*. The interaction list of a given cell at some refinement level s consists of the cells at the same refinement level whose parents are nearest neighbors to the parent of the cell, but which are not themselves nearest neighbors of the cell. The interaction list contains 189 cells. See Fig. 1.

Now we are ready to go through the algorithm. It consists of the following steps:

- compute coefficients for the multipole expansion for each cell at refinement level S.

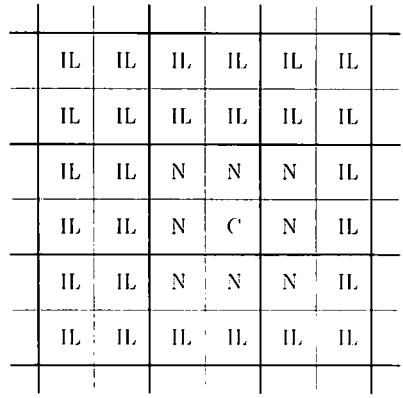

Fig. 1. Two-dimensional cut showing the neigbors (marked N) and the interaction list (marked IL) of the cell, marked C. Thick lines indicate the parent refinement level.

- upward pass—compute coefficients for the multipole expansion for each cell at all refinement levels.
- periodic boundary conditions.
- downward pass—compute coefficients for the local expansion for each cell at all refinement levels.
- direct calculations at refinement level S.

Each step will now be treated in some detail. Before starting the upward pass, coefficients for the multipole expansion are computed for each cell at refinement level S. This multipole expansion describes the potential due to all charges located inside the cell, and it is valid outside the sphere which touches the corners of the cell.

Now the upward pass can begin. It starts at refinement level S. where, for each cell, the center of the multipole expansion is translated to the center of the parent cell. Each parent cell thus "receives" eight translated multipole expansions, which are added, and the result is a new multipole expansion (we will often use the term "adding expansions", although we actually mean combining them by adding their coefficients). The new multipole expansion describes the potential due to all charges inside the parent cell and it is valid outside the sphere which touches the corners of the cell. This process of translating and adding the expansions is repeated until a multipole expansion for the whole computational cell about its center is available.

If periodic boundary conditions are used, then the multipole expansion obtained for the computational cell is also a multipole expansion for

all the identical cells surrounding the computational cell. The multipole expansions from all cells except the computational cell and its nearest neighbors are now converted into local expansions centered at the center of the computational cell and added. If we for a moment assume that the infinite spherical array of cells is surrounded by vacuum, the result is a local expansion describing the potential due to all charges located outside the computational cell and its nearest neighbors and it is valid inside the sphere which touches the corners of the cell. This local expansion is the starting point for the downward pass. The sum mentioned above is infinite, but because of the fact that all the multipole expansions which are converted and added are equal, their coefficients can be taken outside the sum over periodic copies, and the infinite part is just a constant sum

$$S(l, m) = \sum_{\mathbf{n} \in \Omega} \frac{Y_l^m(\hat{\mathbf{n}})}{n^{l+1}}, \qquad l = 1,..., 2L, \quad m = -l,..., l \tag{15}$$

for each coefficient, where

$$\Omega = \{\mathbf{n} = (n_x, n_y, n_z), \text{ where } n_x, n_y, n_z \in \mathbb{Z} \text{ and } |\mathbf{n}| > \sqrt{3}\} \tag{16}$$

These constant sums can be calculated once for all using the chosen summation order (see Introduction).

Consider now the downward pass. At refinement level zero the local expansion is translated to the center of each of the eight children. For each child (we are now at refinement level one) the received local expansion describes the potential from charges located outside the parent cell and the nearest neighbors of the parent cell. What we want is a local expansion describing the potential from charges outside the cell itself and its nearest neighbors. What remain to be added are thus exactly the contributions from the charges located in the cells in the interaction list. By converting the multipole expansion (which was calculated during the upward pass) of each cell in the interaction list to a local expansion centered at the center of the cell and adding, we finally get the local expansion we wanted. This process of translating the local expansion of each cell to its children and then at the next refinement level adding the contributions from the converted multipole expansions of the cells in the interaction list at that level is repeated down to the maximum refinement level S. where the result is a local expansion for each cell describing the potential from all charges outside the cell and its nearest neighbors. Notice that there is not a full interaction list for cells near the boundary of the computational box when periodic boundary conditions are absent. In the presence of periodic boundary conditions, each cell has a full interaction list when applying a three-dimensional toroidal connectivity of the cells.

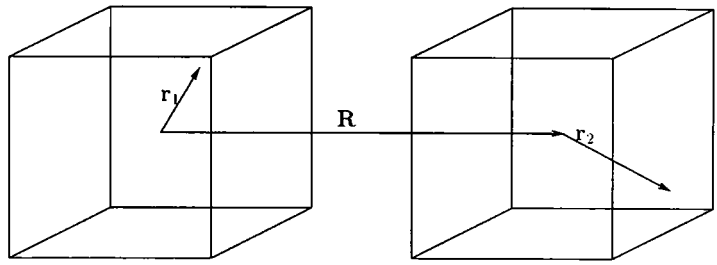

Fig. 2. Configuration of two unit charges in cells separated by **R**.

To get the potential acting on each charge in a given cell from all the charges residing outside the cell and its nearest neighbors, the local expansion is evaluated at the point where the charge is located. The remaining contributions from charges inside the same cell and its nearest neighbors are calculated directly. The forces are obtained in a similar manner.

We have thus found potentials and corresponding forces for the case where the infinite array of cells is surrounded by vacuum. It is well known[4] that correct results for other values ε' of the dielectric constant of the surroundings are found by subtracting

$$\frac{4\pi(\varepsilon'-1)}{3(2\varepsilon'+1)}\left[\sum_{j=1}^{N} q_j \mathbf{r}_j\right]^2$$

from the potential energy obtained for vacuum surroundings. This term and the force contributions derived from it are single-particle sums and may be dealt with separately.

As an illustrative example for which we derive suitable error expressions, we consider now two unit charges positioned in the computational cell so their interaction is subject to approximation, that is, they do not reside in the same cell or in neighbor cells at refinement level S. The configuration is shown in Fig. 2. The two unit charges are positioned in two equally sized cells at positions $\mathbf{r}_1$ and $\mathbf{r}_2$ with respect to the centers of their host cells. These centers are separated by **R**. No matter where in the computational cell the charges are positioned, the configuration in Fig. 2, where each cell is part of the interaction list of the other cell, will occur at some refinement level in the FMM.

We now proceed as in ref. 13.

The potential

$$\phi(\mathbf{R}, \mathbf{r}_1, \mathbf{r}_2) = \frac{1}{|\mathbf{R}+\mathbf{r}_2-\mathbf{r}_1|} \tag{17}$$

can be rewritten as

$$\phi(\mathbf{R}, \mathbf{r}_1, \mathbf{r}_2) = \left\{ |\mathbf{R}+\mathbf{r}_2| \left[1 - 2\frac{|\mathbf{r}_1|}{|\mathbf{R}+\mathbf{r}_2|} (\widehat{\mathbf{R}+\mathbf{r}_2}) \cdot \widehat{\mathbf{r}_1} + \left(\frac{|\mathbf{r}_1|}{|\mathbf{R}+\mathbf{r}_2|} \right)^2 \right]^{1/2} \right\}^{-1} \tag{18}$$

and using

$$\frac{1}{\sqrt{1-2zt+t^2}} = \sum_{l=0}^{\infty} t^l P_l(z) \qquad \text{for} \quad |t| < 1 \tag{19}$$

where $P_l(z)$ is the Legendre polynomial, and in general writing $|\mathbf{r}|$ as r, we get

$$\phi(\mathbf{R}, \mathbf{r}_1, \mathbf{r}_2) = \sum_{l_1=0}^{\infty} \frac{r_1^{l_1}}{|\mathbf{R}+\mathbf{r}_2|^{l_1+1}} P_{l_1}((\widehat{\mathbf{R}+\mathbf{r}_2}) \cdot \widehat{\mathbf{r}_1}) \tag{20}$$

Before going any further, we truncate this expansion to a finite number of terms:

$$\phi(\mathbf{R}, \mathbf{r}_1, \mathbf{r}_2) = \sum_{l_1=0}^{L} \frac{r_1^{l_1}}{|\mathbf{R}+\mathbf{r}_2|^{l_1+1}} P_{l_1}((\widehat{\mathbf{R}+\mathbf{r}_2}) \cdot \widehat{\mathbf{r}_1}) + \mathscr{E}_L(\mathbf{R}, \mathbf{r}_1, \mathbf{r}_2) \tag{21}$$

The Legendre polynomial can be expressed in terms of spherical harmonics using the summation formula for spherical harmonics:

$$P_l(\widehat{\mathbf{r}_1} \cdot \widehat{\mathbf{r}_2}) = \frac{4\pi}{2l+1} \sum_{m=-l}^{l} Y_l^m{}^*(\widehat{\mathbf{r}_1})\, Y_l^m(\widehat{\mathbf{r}_2}) \tag{22}$$

Applying (22), we find that the potential becomes

$$\phi(\mathbf{R}, \mathbf{r}_1, \mathbf{r}_2) = \sum_{l_1=0}^{L} \sum_{m_1=-l_1}^{l_1} \frac{4\pi}{2l_1+1} \frac{Y_{l_1}^{m_1}(\widehat{\mathbf{R}+\mathbf{r}_2})}{|\mathbf{R}+\mathbf{r}_2|^{l_1+1}} Y_{l_1}^{m_1}{}^*(\widehat{\mathbf{r}_1})\, r_1^{l_1} + \mathscr{E}_L(\mathbf{R}, \mathbf{r}_1, \mathbf{r}_2) \tag{23}$$

In fact, (23) is the unique multipole expansion centered at the origin of the potential from charge number one evaluated at the position of charge number two. The expansion is valid outside the cell of charge number one. Independent of the maximum refinement level S, we will arrive at this multipole expansion at the refinement level of Fig. 2 during the upward pass.

Now we can expand

$$\frac{Y_{l_1}^{m_1}(\widehat{\mathbf{R}+\mathbf{r}_2})}{|\mathbf{R}+\mathbf{r}_2|^{l_1+1}}$$

using the following formula, where $\mathbf{s}=\mathbf{R}-\mathbf{r}$ and $|\mathbf{R}|>|\mathbf{r}|$:

$$\frac{Y_{l_1}^{m_1}(\hat{\mathbf{s}})}{s^{l_1+1}}=\sqrt{4\pi}\sum_{l_2=0}^{\infty}\sum_{m_2=-l_2}^{l_2}\frac{(-1)^{m_2}}{2l_2+1}D(l_1,m_1,l_2,m_2)\times Y_{l_2}^{m_2}(\hat{\mathbf{r}})\,r^{l_2}\frac{Y_{l_1+l_2}^{m_1-m_2}(\hat{\mathbf{R}})}{R^{l_1+l_2+1}} \tag{24}$$

where

$$D(l_1,m_1,l_2,m_2)=\frac{V(l_1,m_1)\,V(l_2,m_2)}{V(l_1+l_2,m_1-m_2)} \tag{25}$$

and

$$V(l,m)=\left[\frac{2l+1}{(l+m)!\,(l-m)!}\right]^{-1} \tag{26}$$

We get

$$\phi(\mathbf{R},\mathbf{r}_1,\mathbf{r}_2)=(4\pi)^{3/2}\sum_{l_1=0}^{L}\sum_{m_1=-l_1}^{l_1}\sum_{l_2=0}^{\infty}\sum_{m_2=-l_2}^{l_2}\frac{(-1)^{m_2}}{(2l_1+1)(2l_2+1)}\times D(l_1,m_1,l_2,m_2)\,r_1^{l_1}\,Y_{l_1}^{m_1}{}^*(\widehat{\mathbf{r}_1})\,r_2^{l_2}\,Y_{l_2}^{m_2}(-\widehat{\mathbf{r}_2})\,\frac{Y_{l_1+l_2}^{m_1-m_2}(\hat{\mathbf{R}})}{R^{l_1+l_2+1}}+\mathscr{E}_L(\mathbf{R},\mathbf{r}_1,\mathbf{r}_2) \tag{27}$$

Again we truncate the infinite sum and apply the fact that $Y_l^m(-\hat{\mathbf{r}})=(-1)^l\,Y_l^m(\hat{\mathbf{r}})$:

$$\phi(\mathbf{R},\mathbf{r}_1,\mathbf{r}_2)=(4\pi)^{3/2}\sum_{l_1=0}^{L}\sum_{m_1=-l_1}^{l_1}\sum_{l_2=0}^{\infty}\sum_{m_2=-l_2}^{l_2}\frac{(-1)^{l_2+m_2}}{(2l_1+1)(2l_2+1)}\times D(l_1,m_1,l_2,m_2)\,r_1^{l_1}\,Y_{l_1}^{m_1}{}^*(\widehat{\mathbf{r}_1})\,r_2^{l_2}\,Y_{l_2}^{m_2}(\widehat{\mathbf{r}_2})\,\frac{Y_{l_1+l_2}^{m_1-m_2}(\hat{\mathbf{R}})}{R^{l_1+l_2+1}}+\mathscr{E}_L(\mathbf{R},\mathbf{r}_1,\mathbf{r}_2)+\mathscr{F}_L(\mathbf{R},\mathbf{r}_1,\mathbf{r}_2) \tag{28}$$

$$\equiv\phi(\mathbf{R},\mathbf{r}_1,\mathbf{r}_2)+\mathscr{E}_L(\mathbf{R},\mathbf{r}_1,\mathbf{r}_2)+\mathscr{F}_L(\mathbf{R},\mathbf{r}_1,\mathbf{r}_2) \tag{29}$$

Equation (28) is a local expansion centered at $\mathbf{R}$ of the potential from charge number one evaluated at the position of charge number two. During the rest of the downward pass the center of the local expansion will be translated once at each refinement level, but the value of $\phi(\mathbf{R}, \mathbf{r}_1, \mathbf{r}_2)$ will remain the same. Thus $\mathscr{E}_L(\mathbf{R}, \mathbf{r}_1, \mathbf{r}_2) + \mathscr{F}_L(\mathbf{R}, \mathbf{r}_1, \mathbf{r}_2)$ is the error in the potential when applying the FMM to a system of two charges. In ref. 13 it is shown that $\mathscr{F}_L$ can be written as

$$\mathscr{F}_L(\mathbf{R}, \mathbf{r}_1, \mathbf{r}_2) = \mathscr{E}_L(-\mathbf{R}, \mathbf{r}_2, \mathbf{r}_1) + \mathscr{E}_L^*(\mathbf{R}, \mathbf{r}_1, \mathbf{r}_2) \tag{30}$$

where

$$\mathscr{E}_L^*(\mathbf{R}, \mathbf{r}_1, \mathbf{r}_2) = (4\pi)^{3/2} \sum_{l_1=L+1}^{\infty} \sum_{m_1=-l_1}^{l_1} \sum_{l_2=L+1}^{\infty} \sum_{m_2=-l_2}^{l_2} \frac{(-1)^{m_2}}{(2l_1+1)(2l_2+1)} \times D(l_1, m_1, l_2, m_2)\, r_1^{l_1} Y_{l_1}^{m_1 *}(\hat{\mathbf{r}}_1)\, r_2^{l_2} Y_{l_2}^{m_2}(-\hat{\mathbf{r}}_2)\, \frac{Y_{l_1+l_2}^{m_1-m_2}(\hat{\mathbf{R}})}{R^{l_1+l_2+1}} \tag{31}$$

The total error in the potential energy can thus be written as

$$\mathscr{E}_L^{\text{tot}}(\mathbf{R}, \mathbf{r}_1, \mathbf{r}_2) = \mathscr{E}_L(\mathbf{R}, \mathbf{r}_1, \mathbf{r}_2) + \mathscr{E}_L(-\mathbf{R}, \mathbf{r}_2, \mathbf{r}_1) + \mathscr{E}_L^*(\mathbf{R}, \mathbf{r}_1, \mathbf{r}_2) \tag{32}$$

where

$$\mathscr{E}_L(\mathbf{R}, \mathbf{r}_1, \mathbf{r}_2) = (4\pi)^{3/2} \sum_{l_1=L+1}^{\infty} \sum_{m_1=-l_1}^{l_1} \sum_{l_2=0}^{\infty} \sum_{m_2=-l_2}^{l_2} \frac{(-1)^{m_2}}{(2l_1+1)(2l_2+1)} \times D(l_1, m_1, l_2, m_2)\, r_1^{l_1} Y_{l_1}^{m_1 *}(\hat{\mathbf{r}}_1)\, r_2^{l_2} Y_{l_2}^{m_2}(-\hat{\mathbf{r}}_2)\, \frac{Y_{l_1+l_2}^{m_1-m_2}(\hat{\mathbf{R}})}{R^{l_1+l_2+1}} \tag{33}$$

and where $\mathscr{E}_L^*$ given by (31).

3. ERROR ESTIMATES FOR THE FMM

The main purpose of this section is to derive estimates for δf_{rms} and $\delta f_{\max}$ as functions of the number of subdivisions S and the number of terms in the expansions L. In Section 3.1, we present some basic approximations; in Section 3.2 we formulate the estimates as an S-dependent term times an L-dependent expectation value. The results derived in this section are summarized in Section 4.

3.1. Necessary Approximations and the Formulation of the Estimates

We first consider the necessary approximations, which we use several times. Throughout the derivation of the estimates we use asymptotic results in L. We thus formally assume that $L \gg 1$, although these results actually are very accurate even for small L values. We furthermore occasionally use the approximation $|\mathbf{R}+\mathbf{r}_2| \gg |\mathbf{r}_1|$ (see Fig. 2). Several times we will also have to evaluate an integral of the form

$$\int_{\mathbf{r}\in[-l/2;\, l/2]^3} |f(\mathbf{r})|^2 \, d\mathbf{r} \tag{34}$$

where l is the side length of a cubic box and $f(\mathbf{r}) \equiv f_1(r)\, f_2(\hat{\mathbf{r}})$. The integral can be rewritten as

$$\int_0^{1/2} 4\pi\, |f_1(r)|^2 \, dr \frac{1}{4\pi} \int_{\bigcirc} |f_2(\hat{\mathbf{r}})|^2 \, d\hat{\mathbf{r}} + \int_{1/2}^{\sqrt{3}\,l/2} V(\Omega(r))\, |f_1(r)|^2 \, dr \frac{1}{V(\Omega(r))} \int_{\Omega(r)} |f_2(\hat{\mathbf{r}})|^2 \, d\hat{\mathbf{r}} \tag{35}$$

Here the first term equals the integral over the largest possible sphere which can he contained in the cubic box, and the second term is the integral over the remaining "corners" of the box. To be more precise, $\bigcirc$ denotes the surface of the unit sphere, and $\Omega(r) \subset \bigcirc$ is the subset of all angular values corresponding to the subset of the surface of the sphere of radius r centered at the origin residing inside a cube of side length l also centered at the origin. It ref. 13 an asymptotic estimate of the error as a function of the charge positions is derived. This estimate shows that the error is an oscillating function of the positions with a frequency near $L+1 \gg 1$. As the angular part of the error is oscillating with a frequency near $L+1 \gg 1$ we may assume that the average of the angular part over $\Omega(r)$ is close to the average over the whole sphere. That is,

$$\frac{1}{V(\Omega(r))} \int_{\Omega(r)} |f_2(\hat{\mathbf{r}})|^2 \, d\hat{\mathbf{r}} \approx \frac{1}{4\pi} \int_{\bigcirc} |f_2(\hat{\mathbf{r}})|^2 \, d\hat{\mathbf{r}} \tag{36}$$

Consider now the overall error in the force on particle i for a system with reduced density $\rho^* = \rho\sigma^3$, where σ is the length scale:

$$\Delta\mathbf{f}_i = \left(\frac{\rho^*}{N}\right)^{2/3} q_i \sum_{s=0}^{S} 4^s \sum_{j\in \mathrm{IL}(i,s)} q_j \Psi_L(\boldsymbol{\rho}_{i,s}, \boldsymbol{\rho}_{j,s}, \boldsymbol{\Gamma}_{i,j,s}) \tag{37}$$

where $\psi_L(\rho_{i,s}, \rho_{j,s}, \Gamma_{i,j,s})$ is the error in the force acting on particle i due to the charge of particle j and IL(i, s) is the interaction list of the host cell of particle i at refinement level s, and where $\rho_{i,s}$ and $\rho_{j,s}$ are the positions of particle i and j with respect to the center of their host cells at level s, and $\Gamma_{i,j,s}$ denotes the displacement of the two host cells ($\rho_{i,s}$, $\rho_{j,s}$ and $\Gamma_{i,j,s}$ are scaled with respect to the cell size at level s). Notice that ψ_L does not depend on S, only on L.

The overall error δf_{rms} may then be written as

$$\delta f_{\text{rms}} = \left(\frac{1}{N} \sum_{i=1}^{N} \Delta \mathbf{f}_i^2 \right)^{1/2} \tag{38}$$

To find an estimate for δf_{rms} we first estimate $\langle \Delta \mathbf{f}_i^2 \rangle$, the expectation value of $\Delta \mathbf{f}_i^2$ for a given position of particle i averaged over all allowed positions for all the particles j which are in IL(i, s) for some s.

To proceed, we assume without proof that

$$\sum_{\Gamma} \langle \psi_L(\mathbf{a}, \mathbf{x}, \Gamma) \rangle_{\mathbf{x}} \approx 0 \qquad \text{for any} \quad \mathbf{a} \tag{39}$$

where $\langle A \rangle_{[subscript]}$ denotes the expectation value of A averaged over the allowed range of the variables in the [*subscript*], and $\sum_{\Gamma}$ is the sum over all cells in the interaction list of the particle located at $\mathbf{a}$.

We furthermore assume that all error contributions are statistically independent. That is, the charges are uncorrelated with respect to positions in space. For simplicity, we further assume that $|q_j| \equiv q$ for all particles $j = 1, \ldots, N$. We then immediately find that

$$\langle \Delta \mathbf{f}_i^2 \rangle = q^4 \frac{(\rho^*)^{4/3}}{N^{1/3}} \sum_{s=0}^{S} 2^s \sum_{\Gamma} \langle \psi_L(\rho_{i,s}, \mathbf{x}, \Gamma)^2 \rangle_{\mathbf{x}} \tag{40}$$

and we can estimate δf_{rms} by

$$\delta f_{\text{rms}} \approx \sqrt{2}\,(\rho^*)^{2/3} q^2 \left(\frac{8^S}{N} \right)^{1/6} \left\{ \sum_{\Gamma} \langle \psi_L(\mathbf{a}, \mathbf{x}, \Gamma)^2 \rangle_{\mathbf{a},\mathbf{x}} \right\}^{1/2} \tag{41}$$

and $\delta f_{\max}$ by

$$\delta f_{\max} \approx \sqrt{2}\,(\rho^*)^{2/3} q^2 \left(\frac{8^S}{N} \right)^{1/6} \left\{ \max_{\mathbf{a}} \left(\sum_{\Gamma} \langle \psi_L(\mathbf{a}, \mathbf{x}, \Gamma)^2 \rangle_{\mathbf{x}} \right) \right\}^{1/2} \tag{42}$$

We have thus already explicitly obtained the S dependence of the errors. To get the L dependence and the overall estimate, we just need to find

$\sum_\Gamma \langle \psi_L(\mathbf{a}, \mathbf{x}, \Gamma)^2 \rangle_{\mathbf{a},\mathbf{x}}$ and $\max_{\mathbf{a}}(\sum_\Gamma \langle \psi_L(\mathbf{a}, \mathbf{x}, \Gamma)^2 \rangle_{\mathbf{x}})$. This is done in the next section.

3.2. Dependence on L and the Overall Estimate

As outlined in Section 2, the total erior in the potential energy due to two unit charges residing as in Fig. 2 can be written as

$$\mathscr{E}_L^{\text{tot}}(\mathbf{R}, \mathbf{r}_1, \mathbf{r}_2) = \mathscr{E}_L(\mathbf{R}, \mathbf{r}_1, \mathbf{r}_2) + \mathscr{E}_L(-\mathbf{R}, \mathbf{r}_2, \mathbf{r}_1) + \mathscr{E}_L^*(\mathbf{R}, \mathbf{r}_1, \mathbf{r}_2) \tag{43}$$

The function $\mathscr{E}_L(\mathbf{R}, \mathbf{r}_1, \mathbf{r}_2)$ can be written as[13]

$$\mathscr{E}_L(\mathbf{R}, \mathbf{r}_1, \mathbf{r}_2) \equiv \delta_L(\mathbf{R}, \mathbf{r}_1, \mathbf{r}_2) \tag{44}$$

where

$$\delta_L(\mathbf{s}, \mathbf{r}) = \sum_{l=L+1}^{\infty} \frac{r^l}{s^{l+1}} P_l(\hat{\mathbf{s}} \cdot \hat{\mathbf{r}}) \tag{45}$$

Assuming that the three contributions in (43) are independent, we can consider the contribution to the rms error from each term in turn. In Appendix B we show that the contribution from $\mathscr{E}_L^*(\mathbf{R}, \mathbf{r}_1, \mathbf{r}_2)$ is negligible compared to the one from $\mathscr{E}_L(\mathbf{R}, \mathbf{r}_1, \mathbf{r}_2)$.

We now turn our attention toward the search for the L dependence in the force error. As $\mathscr{E}_L^*$ contribution was negligible, we assume that the corresponding force errors from $\mathscr{E}_L^*$ negligible as well. We can then write the the error on the force on the charge at $\mathbf{r}_2$ from the $\mathbf{r}_1 - \mathbf{r}_2$ interaction as

$$\mathbf{f}(\mathbf{r}_2) = \frac{\partial \mathscr{E}_L^{\text{tot}}}{\partial \mathbf{r}_2} \approx \frac{\partial(\delta_L(\mathbf{R} + \mathbf{r}_2, \mathbf{r}_1))}{\partial \mathbf{r}_2} + \frac{\partial(\delta_L(-\mathbf{R} + \mathbf{r}_1, \mathbf{r}_2))}{\partial \mathbf{r}_2} \tag{46}$$

By observing that

$$\frac{\partial(\delta_L(\mathbf{s}, \mathbf{r}))}{\partial \mathbf{r}} = \sum_{l=L+1}^{\infty} \frac{r^{l-1}}{s^{l+1}} \left[\hat{\mathbf{r}} l P_l(\hat{\mathbf{s}} \cdot \hat{\mathbf{r}}) + (\hat{\mathbf{s}} - (\hat{\mathbf{s}} \cdot \hat{\mathbf{r}})\, \hat{\mathbf{r}}) \frac{d}{dz} P_l(z) \right] \tag{47}$$

and

$$\frac{\partial(\delta_L(\mathbf{s}, \mathbf{r}))}{\partial \mathbf{s}} = \sum_{l=L+1}^{\infty} \frac{r^l}{s^{l+2}} \left[-\hat{\mathbf{s}}(l+1) P_l(\hat{\mathbf{s}} \cdot \hat{\mathbf{r}}) + (\hat{\mathbf{r}} - (\hat{\mathbf{s}} \cdot \hat{\mathbf{r}})\, \hat{\mathbf{s}}) \frac{d}{dz} P_l(z) \right] \tag{48}$$

where $z = \hat{\mathbf{s}} \cdot \hat{\mathbf{r}}$, and assuming again that $s^2 \gg r^2$, we observe that the second expression is negligible compared to the first and then

$$|\mathbf{f}(\mathbf{r})|^2 \approx \left| \sum_{l=L+1}^{\infty} \frac{r^{l-1}}{s^{l+1}} \left[\hat{\mathbf{r}} l P_l(z) + (\hat{\mathbf{s}} - z\hat{\mathbf{r}}) \frac{d}{dz} P_l(z) \right] \right|^2 \tag{49}$$

$$= \left[\sum_{l=L+1}^{\infty} \frac{r^{l-1}}{s^{l+1}} l P_l(z) \right]^2 + \left[\sum_{l=L+1}^{\infty} \frac{r^{l-1}}{s^{l+1}} P_l^1(z) \right]^2 \tag{50}$$

By using the following result for associated Legendre polynomials

$$\int_{-1}^{1} P_n^m(z)\, P_k^m(z)\, dz = \begin{cases} 0 & \text{if } n \neq k \\ \dfrac{2}{2n+1} \dfrac{(n+m)!}{(n-m)!} & \text{if } n = k \end{cases} \tag{51}$$

we obtain

$$\begin{aligned} \langle |\mathbf{f}(\mathbf{r})|^2 \rangle_{\hat{\mathbf{s}}, \hat{\mathbf{r}}} &= \sum_{l=L+1}^{\infty} \frac{r^{2(l-1)}}{s^{2(l-1)}} l^2 \frac{1}{2l+1} + \sum_{l=L+1}^{\infty} \frac{r^{2(l-1)}}{s^{2(l-1)}} (l+1)\, l \\ &= \sum_{l=L+1}^{\infty} \frac{r^{2(l-1)}}{s^{2(l-1)}} \\ &\approx (L+1) \frac{r^{2L}}{s^{2(L+2)}} \end{aligned} \tag{52}$$

where we have used $L+1 \gg 1$ and $s^2 \gg r^2$ to get the last approximation. By using the results in Appendix B, Eqs. (B4) and (B5), we get the overall error estimate from all the particles in the interaction list at a given level as

$$\left\{ \sum_{\Gamma} \langle \psi_L(\mathbf{a}, \mathbf{x}, \Gamma)^2 \rangle_{\mathbf{a}, \mathbf{x}} \right\}^{1/2} \approx \frac{27\pi}{2} \frac{1}{(L+1/2)\sqrt{L(L+1)}} \left(\frac{\sqrt{3}}{3} \right)^L \tag{53}$$

Similarly, we can find the L dependence of the maximum error, where we again arrive at (52), and then

$$\left\{ \max_{\mathbf{a}} \left(\sum_{\Gamma} \langle \psi_L(\mathbf{a}, \mathbf{x}, \Gamma)^2 \rangle_{\mathbf{x}} \right) \right\}^{1/2} \approx \frac{\sqrt{2\pi}}{\sqrt{L+1/2}} \left(\frac{\sqrt{3}}{3} \right)^L \tag{54}$$

4. MODELS FOR THE ERRORS

In the previous section we obtained theoretical estimates for the expected errors in the case of no correlations. The estimates were expressed

as functions of the parameters of the FMM, that is, the number of terms in the expansions L and the number of subdivisions of the computational box S. Now we can make a model for the expected error, again as a function of L and S.

Assuming that the user measures the charge size q in units of elementary charge e, and that the user has chosen a length scale σ, the model of the error δf_{rms} in units of (e^2/σ^2) is

$$\delta f_{\text{rms}}^{\text{nocorr}} \left(\frac{27\pi}{2}\right)^{1/2} (\rho^*)^{2/3} q^2 \left(\frac{8^S}{N}\right)^{1/6} \frac{1}{(L+1/2)\sqrt{L(L+1)}} \left(\frac{\sqrt{3}}{3}\right)^L \tag{55}$$

where N is the total number of charges and $\rho^* = \rho\sigma^3$ is the so-called reduced density for the given absolute density ρ.

We have based all estimates on the assumption that the charges and their positions are statistically uncorrelated. However, some correlation must be expected due to screening effects. In terms on the length of a given cell at some level s, the length of these correlations must be expected to be proportional to $(N/8^S)^{-1/3}$. This length should be compared to the effective wavelength of the oscillating functions which describe the error. These wavelengths are, as previously meritioned, approximately proportional to $1/(L+1)$. Based on these observations, we assume that the correlations will yield a factor which is a function depending on the single variable $x = N^{1/3}/2^S(L+1)$. We thus arrive at our final estimate for δf_{rms}:

$$\begin{aligned}\delta f_{\text{rms}} = &\left(\frac{27\pi}{2}\right)^{1/2} (\rho^*)^{2/3} q^2 \left(\frac{8^S}{N}\right)^{1/6} \frac{1}{(L+1/2)\sqrt{L(L+1)}} \\ &\times \left(\frac{\sqrt{3}}{3}\right)^L \Phi\left(\frac{N^{1/3}}{2^S(L+1)}\right)\end{aligned} \tag{56}$$

where we expect $\Phi(x) \to 1$ as $x \to 0$ (that is, as the charges become uncorrelated) and that $\Phi(x) \to 0$ as $x \to \infty$.

Independent of the correlations, we expect a maximum to average error ration

$$\frac{\delta f_{\max}}{\delta f_{\text{rms}}} = \left[\frac{8}{27} L\left(L+\frac{1}{2}\right)(L+1)\right]^{1/2} \tag{57}$$

5. RESULTS AND DISCUSSION

In this section we will compare the derived theoretical models for the errors from Section 4 to errors found experimentally.

We use two systems containing 10,000 and 100,000 charges. The test system is a simple model of molten salt, NaCl. Ions are represented by Lennard-Jones particles carrying plus or minus elementary charge. The LJ parameters are given in Table I, (taken from ref. 1), where the Lennard-Jones interaction is

$$U_{LJ}(r) = 4\varepsilon[(\sigma/r)^{12} - (\sigma/r)^6] \tag{58}$$

The configurations were prepared by the molecular dynamics method. The initial configuration was a crystal with randomly distributed ions and some (randomly distributed) vacancies. The density was 2.4 g cm^{-3}. From this high-energy configuration the system was cooled to temperature $T = 2000$ K and further equilibrated. The simulation times (about 1 psec for the $N = 10000$ system and 0.5 psec for $N = 100000$) were not sufficient to equilibrate the global charge distribution, but were enough to create local charge distribution and liquid structure.

For the equilibrated systems, we calculate the forces by the Ewald method using very high accuracy (relative errors around 10^{-10}). These forces were used $\mathbf{f}_i^{\text{exact}}$. We then calculated the forces using the FMM for various L and S values.

In the following presentation, we have decided to present the results for the errors both in tables and figures. The reason is that error comparisons among FMM users are much easier when tables of errors are available, whereas the figures are necessary for a qualitative understanding.

Tables II and III list the measured ε_{rms}, the no-correlation estimate $\delta f_{\text{nocorr rms}}/f_{\text{rms}}$ for ε_{rms}, the measured $\varepsilon_{\max}$, the measured $\delta f_{\max}/\delta f_{\text{rms}}$ and finally the estimated $\delta f_{\max}/\delta f_{\text{rms}}$ as functions of L and S for the two systems studied.

First, we observe that the ratio $\delta f_{\max}/\delta f_{\text{rms}}$ has the expected strong L dependence. The huge values of $\delta f_{\max}/\delta f_{\text{rms}}$ for accurate FMM simulations is a serious drawback of the method. Figures 3 and 4 plot the measured and estimated values for different S. As expected, there is no S dependence. The differences are due to fluctuations in $\delta f_{\max}$.

Table I. Lennard–Jones Parameters for Molten Salt Test System[a]

Pair	σ (Å)	ε (cal $mole^{-1}$)
Na^+, Na^+	3.64912	6.5
Cl^-, Cl^-	3.61705	60
Na^+, Cl^-	3.63308	16.23

[a] Taken from ref. 1.

Table II. Errors for $N = 10{,}000$[a]

L	S	ε_{rms}	$\delta f_{\text{rms}}^{\text{nocorr}}/f_{\text{rms}}$	ε_{max}	$\delta f_{\text{max}}/\delta f_{\text{rms}}$	$(\delta f_{\text{max}}/\delta f_{\text{rms}})_{\text{exp}}$
3	1	4.10e-3	3.56e-2	1.91e-2	4.66	3.16
4	1	2.13e-3	1.20e-2	1.16e-2	5.44	4.80
5	1	1.00e-3	4.51e-3	6.70e-3	6.68	6.63
6	1	4.52e-4	1.83e-3	3.69e-3	8.16	8.60
7	1	2.31e-4	7.86e-4	3.53e-3	15.31	10.77
8	1	1.16e-4	3.50e-4	1.78e-3	15.39	13.04
9	1	4.66e-5	1.61e-4	5.47e-4	11.72	15.49
10	1	2.66e-5	7.55e-5	3.69e-4	13.72	18.03
3	2	1.13e-2	5.04e-2	6.01e-2	5.30	3.16
4	2	5.04e-3	1.69e-2	2.98e-2	5.91	4.80
5	2	2.33e-3	6.38e-3	1.47e-2	6.34	6.63
6	2	1.08e-3	2.59e-3	9.15e-3	8.50	8.60
7	2	4.81e-4	1.11e-3	4.48e-3	9.31	10.77
8	2	2.38e-4	4.95e-4	2.82e-3	11.83	13.04
9	2	1.08e-4	2.27e-4	1.50e-3	13.81	15.49
10	2	5.43e-5	1.07e-4	8.61e-4	15.84	18.03
3	3	2.36e-2	7.13e-2	1.16e-1	4.90	3.16
4	3	1.03e-2	2.39e-2	6.13e-2	5.94	4.80
5	3	4.73e-3	9.02e-3	3.96e-2	8.36	6.63
6	3	2.19e-3	3.67e-3	2.16e-2	9.88	8.60
7	3	1.00e-3	1.57e-3	1.54e-2	15.42	10.77
8	3	4.74e-4	7.00e-4	4.88e-3	10.28	13.04
9	3	2.19e-4	3.21e-4	2.53e-3	11.59	15.49
10	3	1.07e-4	1.51e-4	1.75e-3	16.40	18.03
3	4	4.52e-2	1.01e-1	2.08e-1	4.60	3.16
4	4	1.98e-2	3.38e-2	1.40e-1	7.06	4.80
5	4	8.89e-3	1.28e-2	9.19e-2	10.33	6.63
6	4	4.12e-3	5.19e-3	3.28e-2	7.95	8.60
7	4	1.87e-3	2.22e-3	2.19e-2	11.73	10.77
8	4	8.92e-4	9.90e-4	9.97e-3	11.18	13.04
9	4	3.97e-4	4.55e-4	5.09e-3	12.83	15.49
10	4	1.99e-4	2.14e-4	3.56e-3	17.93	18.03

[a] The exact potential energy was 3681.564059195 and $f_{\text{rms}} = 0.138882767180194$.

Table III. Errors for $N = 100{,}000$[a]

L	S	ε_{rms}	$\delta f_{\text{rms}}^{\text{nocorr}}/f_{\text{rms}}$	ε_{max}	$\delta f_{\text{max}}/\delta f_{\text{rms}}$	$(\delta f_{\text{max}}/\delta f_{\text{rms}})_{\text{exp}}$
3	2	5.02e-3	3.39e-2	2.78e-2	5.53	3.16
4	2	2.24e-3	1.14e-2	1.51e-2	6.75	4.80
5	2	1.01e-3	4.28e-3	9.49e-3	9.36	6.63
6	2	4.60e-4	1.74e-3	3.89e-3	8.46	8.60
7	2	2.30e-4	7.47e-4	2.68e-3	11.62	10.77
8	2	1.07e-4	3.33e-4	1.98e-3	18.60	13.04
9	2	5.07e-5	1.53e-4	8.78e-4	17.29	15.49
10	2	2.41e-5	7.18e-5	4.77e-4	19.80	18.03
3	3	1.07e-2	4.79e-2	6.02e-2	5.65	3.16
4	3	4.66e-3	1.61e-2	2.97e-2	6.37	4.80
5	3	2.12e-3	6.06e-3	1.63e-2	7.68	6.63
6	3	9.75e-3	2.46e-3	9.56e-3	9.81	8.60
7	3	4.64e-4	1.06e-3	6.45e-3	13.91	10.77
8	3	2.18e-4	4.70e-4	3.24e-3	14.91	13.04
9	3	1.02e-4	2.16e-4	1.60e-3	15.63	15.49
10	3	4.88e-5	1.01e-4	8.98e-4	18.39	18.03
3	4	2.15e-2	6.77e-2	1.10e-1	5.13	3.16
4	4	9.37e-3	2.27e-2	6.66e-2	7.11	4.80
5	4	4.24e-3	8.57e-3	3.52e-2	8.31	6.63
6	4	1.95e-3	3.48e-3	2.10e-2	10.74	8.60
7	4	9.03e-4	1.49e-3	1.07e-2	11.84	10.77
8	4	4.20e-4	6.65e-4	6.26e-3	14.91	13.04
9	4	1.95e-4	3.05e-4	2.87e-3	14.70	15.49
10	4	9.33e-5	1.44e-4	1.83e-3	19.60	18.03
3	5	4.23e-2	9.58e-2	2.54e-1	6.01	3.16
4	5	1.83e-2	3.21e-2	1.42e-1	7.78	4.80
5	5	8.04e-3	1.21e-2	8.01e-2	9.96	6.63
6	5	3.68e-3	4.93e-3	4.63e-2	12.58	8.60
7	5	1.71e-3	2.11e-3	2.53e-2	14.78	10.77
8	5	7.92e-4	9.41e-4	1.48e-2	18.63	13.04
9	5	3.68e-4	4.32e-4	6.36e-3	17.27	15.49
10	5	1.77e-4	2.03e-4	3.43e-3	19.32	18.03

[a] The exact potential energy was 36849.35230253 and $f_{\text{rms}} = 0.1408438522961307$.

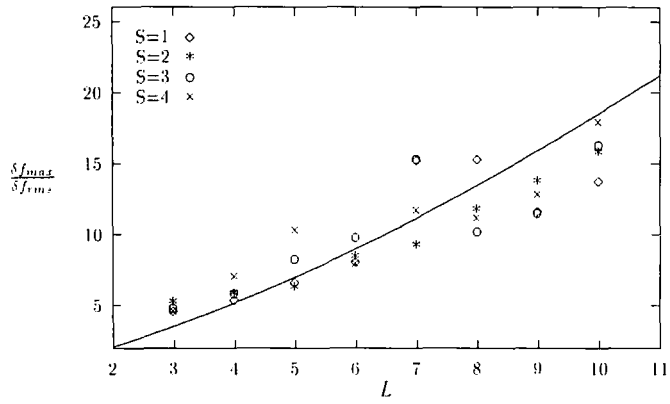

Fig. 3. The ratio for $\delta f_{\max}/\delta f_{\text{rms}}$ $N = 10,000$.

Considering the columns with ε_{rms} and $\delta f_{\text{nocorrrms}}/f_{\text{rms}}$, we make several observations. The first is to notice that the measured error is smaller than the no-correlation estimate. Thus we have correlations in our systems, just as we would expect. Furthermore, we observe that ε_{rms} and $\delta f_{\text{nocorrrms}}/f_{\text{rms}}$ move closer as S increases. This is very reasonable because when S increases (for fixed N) the function Φ in Eq. (56) tends to 1. In order to get a picture of the correlation function Φ defined in Section 4, we plot

$$\frac{\delta f_{\text{rms}}}{\delta f_{\text{nocorrrms}}} = \varepsilon_{\text{rms}} \Big/ \frac{\delta f_{\text{nocorrrms}}}{f_{\text{rms}}}$$

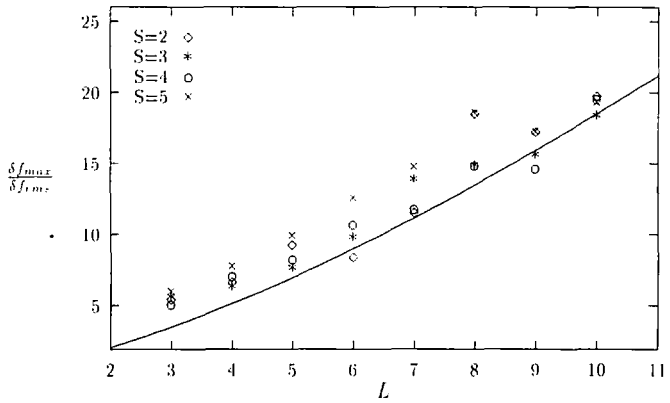

Fig. 4. The ratio for $\delta f_{\max}/\delta f_{\text{rms}}$ $N = 100,000$.

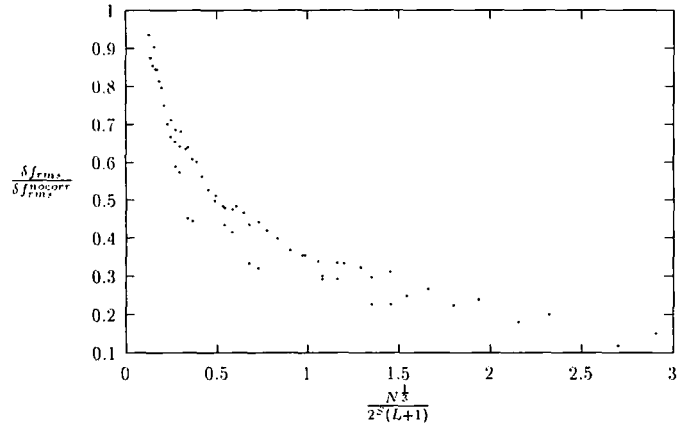

Fig. 5. Experimentally found values for the correlation function $\Phi(N^{1/3}/2^S(L+1))$.

as function of $x = N^{1/3}/2^S(L+1)$ (see Fig. 5). It is strongly indicated that the correlations indeed can be measured by the single variable $x = N^{1/3}/2^S(L+1)$. The measured $\Phi(x)$ tends to one as x becomes small. This strongly indicates that our error estimate (56) is very accurate. In practice $x = N^{1/3}/2^S(L+1)$ will be in the range from 0.3 to 1 for an efficient choice of S. Thus the errors are reduced by a factor of 0.3–0.7 due to correlations.

6. CONCLUSION AND PERSPECTIVES

We have derived an estimate of the root mean square force error for the fast multipole method. The estimate has been demonstrated to be very precise. It is of the form (56),

$$\delta f_{\text{rms}} = \Psi\left(\rho^*, q, L, \frac{N}{8^S}\right) \Phi\left(\frac{N^{1/3}}{2^S(L+1)}\right) \tag{59}$$

An analytic expression was found for the function Ψ, which denotes the root mean square error when no correlations are present. Several important observations can be obtained from this function. First, there is no proper geometric factor for realistic L values. The decrease in error as L increases is due to the factor $(\sqrt{3}/3)^L$ as well as the L dependent coefficient. In the limit as $L \to \infty$, the geometric factor is 3/4,[13] but this is more of mathematical interest than of practical use. Another observation is that the error also depends on S (for fixed N). This is of importance when tuning the method (see below).

We have not been able to find an analytic expression for the function $\Phi(x)$ responsible for correlations. However, $\Phi(x)$ has been properly demonstrated experimentally in Fig. 5, and it was observed that $\Phi(x) \to 1$ as $x \to 0$ (no correlations), thus validating the no correlation estimate.

There are several perspectives which derive from having found these estimates apart from a better understanding of the method. We shall below briefly discuss one perspective, namely with respect to parameter tuning.

In a reliable simulation one should decide in advance the accuracy at which the simulation should be run. Taking this required accuracy as input together with the system parameters N, q, and ρ^*, it is possible to find optimal parameters L and S by solving the constrained optimization problem

$$\min T(N, L, S) \tag{60}$$

$$\text{subject to } \varepsilon = \Psi\left(\rho^*, q, L, \frac{N}{8^S}\right) \Phi\left(\frac{N^{1/3}}{2^S(L+1)}\right) \tag{61}$$

where T is the overall computation time as function of N, L, and S,[11] and ε is the required accuracy (given as a root mean square force error). Thus parameters L and S which ensure maximal efficiency and accuracy can be predicted theoretically.

APPENDIX A. THEOREMS FOR EXPANSION MANIPULATION

Theorem A1 (Making a multipole expansion). Assume that n particles are located at positions $\mathbf{r}_i$ having charges q_i, $i = 1,..., n$, and $|\mathbf{r}_i| < C$. The multipole expansion of the potential at the point $\mathbf{R}$, $|\mathbf{R}| > C$, is then

$$\phi(\mathbf{R}) = \sum_{l=0}^{\infty} \sum_{m=-l}^{l} A_l^m \frac{Y_l^m(\hat{\mathbf{R}})}{R^{l+1}}$$

where

$$A_l^m = \frac{4\pi}{2l+1} \sum_{i=1}^{n} q_i r_i^l Y_l^{m*}(\hat{\mathbf{r}}_i)$$

The expansion is valid outside the sphere with radius C.

Theorem A2 (Translating the center of a multipole expansion). Assume that we have a multipole expansion centered at the point $\mathbf{r}_0$. The

expansion is valid outside a sphere with center $\mathbf{r}_0$ and radius C. Then for any point $\mathbf{R}$ where $|\mathbf{R}-\mathbf{r}_0| > C$

$$\phi(\mathbf{R}) = \sum_{l=0}^{\infty} \sum_{m=-l}^{l} A_l^m \frac{Y_l^m(\widehat{\mathbf{R}-\mathbf{r}_0})}{|\mathbf{R}-\mathbf{r}_0|^{l+1}}$$

The center of this multipole expansion can be translated to the origin, and it will then be valid for any point $\mathbf{R}$ where $|\mathbf{R}| > |\mathbf{r}_0| + C$,

$$\phi(\mathbf{R}) = \sum_{l_1=0}^{\infty} \sum_{m_1=-l_1}^{l} B_{l_1}^{m_1} \frac{Y_{l_1}^{m_1}(\hat{\mathbf{R}})}{R^{l_1+1}}$$

where

$$B_{l_1}^{m_1} = \sqrt{4\pi} \sum_{l_2=0}^{l_1} \sum_{m_2=-l_2}^{l_2} \frac{(-1)^{m_2}}{2l_2+1} A_{l_1-l_2}^{m_1+m_2} \times D(l_1-l_2, m_1+m_2, l_2, m_2)\, Y_{l_2}^{m_2}(\widehat{\mathbf{r}_0})\, r_0^{l_2}$$

and $D(l_1-l_2, m_1+m_2, l_2, m_2)$ is defined in (25).

Theorem A3 (Converting a multipole expansion to a local expansion). Assume that we have a multipole expansion centered at the point $\mathbf{r}_0$ and $|\mathbf{r}_0| > 2C$. The expansion is valid outside a sphere with center $\mathbf{r}_0$ and radius C. Then for any point $\mathbf{R}$ where $|\mathbf{R}-\mathbf{r}_0| > C$

$$\phi(\mathbf{R}) = \sum_{l=0}^{\infty} \sum_{m=-l}^{l} A_l^m \frac{Y_l^m(\widehat{\mathbf{R}-\mathbf{r}_0})}{|\mathbf{R}-\mathbf{r}_0|^{l+1}}$$

This multipole expansion can be converted into a local expansion centered at the origin and valid inside the sphere with center at the origin and radius C. Then for points $\mathbf{R}$ where $|\mathbf{R}| < C$

$$\phi(\mathbf{R}) = \sum_{l_1=0}^{\infty} \sum_{m_1=-l_1}^{l_1} B_{l_1}^{m_1} Y_{l_1}^{m_1}(\hat{\mathbf{R}})\, R^{l_1}$$

where

$$B_{l_1}^{m_1} = (-1)^{m_1} \frac{\sqrt{4\pi}}{2l_1+1} \sum_{l_2=0}^{\infty} \sum_{m_2=-l_2}^{l_2} (-1)^{l_2} A_{l_2}^{m_2} D(l_2, m_2, l_1, m_1) \frac{Y_{l_1+l_2}^{m_2-m_1}(\widehat{\mathbf{r}_0})}{r_0^{l_1+l_2+1}}$$

and $D(l_2, m_2, l_1, m_1)$ is defined in (25).

Theorem A4 (Translating the center of a local expansion). Assume that we have a local expansion centered at the point $\mathbf{r}_0$. The expansion is

valid inside the sphere with center $\mathbf{r}_0$ and radius C, $C > |\mathbf{r}_0|$. Then for any point $\mathbf{R}$ where $|\mathbf{R}-\mathbf{r}_0| > C$

$$\phi(\mathbf{R}) = \sum_{l=0}^{\infty} \sum_{m=-l}^{l} B_l^m Y_l^m(\widehat{\mathbf{R}-\mathbf{r}_0}) \, |\mathbf{R}-\mathbf{r}_0|^l$$

The center of this local expansion can be translated to the origin, and will then be valid for any point $\mathbf{R}$ where $|\mathbf{R}| < C - |\mathbf{r}_0|$,

$$\phi(\mathbf{R}) = \sum_{l_1=0}^{\infty} \sum_{m_1=-l_1}^{l_1} C_{l_1}^{m_1} Y_{l_1}^{m_1}(\hat{\mathbf{R}}) \, R^{l_1}$$

where

$$C_{l_1}^{m_1} = \sqrt{4\pi}\,(-1)^{l_1} \sum_{l_2=l_1}^{\infty} \sum_{m_2=-l_2}^{l_2} \frac{(-1)^{l_2}}{2(l_2-l_1)+1} \times B_{l_2}^{m_2} E(l_2, m_2, l_2-l_1, m_2-m_1) \, Y_{l_2-l_1}^{m_2-m_1}(\widehat{\mathbf{r}_0})$$

and

$$E(l_1, m_1, l_2, m_2) = \frac{2l_1+1}{2(l_1-l_2)+1} \frac{V(l_1-l_2, m_1-m_2) \, V(l_2, m_2)}{V(l_1, m_1)}$$

where $V(l, m)$ is defined in (26).

APPENDIX B. $\mathscr{E}_L$ VERSUS $\mathscr{E}_L^*$

We will show that the contribution to the error in the potential from $\mathscr{E}_L^*$ is negligible compared to the contribution from $\mathscr{E}_L$.

First we consider $\mathscr{E}_L(\mathbf{R}, \mathbf{r}_1, \mathbf{r}_2) \equiv \delta_L(\mathbf{R}+\mathbf{r}_2, \mathbf{r}_1)$. We have

$$\langle \delta_L(\mathbf{s}, \mathbf{r})^2 \rangle_{\hat{\mathbf{s}}, \hat{\mathbf{r}}} = \sum_{l=L+1}^{\infty} \frac{r^{l_2}}{s^{2(l+1)}} \frac{1}{2l+1} \tag{B1}$$

where we have used the fact that

$$\int_{-1}^{1} P_{l_1}(z) \, P_{l_2}(z) \, dz = \begin{cases} 0 & \text{if } l_1 \neq l_2 \\ \dfrac{2}{2l_1+1} & \text{if } l_1 = l_2 \end{cases} \tag{B2}$$

Assuming that $L \gg 1$ and $s^2 \gg r^2$, we get

$$\langle \delta_L(\mathbf{s}, \mathbf{r})^2 \rangle_{\hat{\mathbf{s}}, \hat{\mathbf{r}}} = \frac{1}{2l+1} \frac{r^{2(L+1)}}{s^{2(L+2)}} \tag{B3}$$

To obtain an estimate for δ_L^2 also averaged over the lengths R, r_1 and r_2 we use the following asymptotic results in L:

$$\langle |\mathbf{y}|^{2L} \rangle_{\mathbf{y} \in [-1/2;\, 1/2]^3} \approx \frac{27}{8L(L+1/2)(L+1)} \left(\frac{\sqrt{3}}{2} \right)^{2L} \tag{B4}$$

and

$$\sum_{\boldsymbol{\Gamma}} \langle |\boldsymbol{\Gamma} + \mathbf{y}|^{-2(L+2)} \rangle_{\mathbf{y} \in [-1/2;\, 1/2]^3} \approx \frac{2\pi}{(L+1/2)(L+1)} \left(\frac{3}{2} \right)^{2L} \tag{B5}$$

Both these estimates have relative errors within 10% for $L \geqslant 3$. We then get

$$\langle \delta_L(\mathbf{s}, \mathbf{r})^2 \rangle_{\mathbf{s}, \mathbf{r}} \approx \frac{243}{32} \frac{\pi}{(L+1)^3 (L+1/2)(L+3/2)(L+2)} \left(\frac{\sqrt{3}}{3} \right)^{2(L+1)} \tag{B6}$$

where we again have used the assumptions that $L \gg 1$ and $s^2 \gg r^2$. We now wish to show that the corresponding $\mathscr{E}_L^*$ contribution is negligible. Starting from (31) and using the facts that the Y_l^m are orthonormal and

$$\sum_{m_1=-l_1}^{l_1} \sum_{m_2=-l_2}^{l_2} \frac{D^2(l_1, m_1, l_2, m_2)}{(2l_1+1)^2 (2l_2+1)^2} = \frac{(2l_1+2l_2)!}{(2l_1+1)!\,(2l_2+1)!} \tag{B7}$$

we find that

$$\begin{aligned} \langle |\mathscr{E}_L^*|^2 \rangle_{\hat{\mathbf{r}}_1, \hat{\mathbf{r}}_2, \hat{\mathbf{R}}} &= \sum_{l_1=L+1}^{\infty} \sum_{l_2=L+1}^{\infty} \frac{(2l_1+2l_2)!}{(2l_1+1)!\,(2l_2+1)!} r_1^{2l_1} r_2^{2l_2} R^{-2(l_1+l_2+1)} \\ &= \sum_{l_1=L+1}^{\infty} \sum_{l_2=L+1}^{\infty} \frac{1}{r_1 r_2 R} \left[\int_0^{r_1} x_1^{2l_1}\, dx_1 \int_0^{r_2} x_2^{2l_2}\, dx_2 \right] \\ &\quad \times \frac{(2l_1+2l_2)!}{(2l_1)!\,(2l_2)!} R^{-2(l_1+l_2)-1} \end{aligned} \tag{B8}$$

We notice that

$$\frac{(2l_1+2l_2)!}{(2l_1)!\,(2l_2)!}R^{-2(l_1+l_2)-1}=\frac{1}{(2l_2)!}\frac{d^{2l_2}}{dR^{2l_2}}\frac{1}{R^{2l_1+1}}$$

$$=\frac{1}{2\pi i}\int_{C_0^{R/2}}\frac{1}{t^{2l_2+1}(t+R)^{2l_1+1}}\,dt$$

$$=\frac{1}{2\pi i}\left(\frac{2}{R}\right)^{2l_1+2l_2+1}\int_{C_0^1}\frac{1}{t^{2l_2+1}(t+2)^{2l_1+1}}\,dt \qquad \text{(B9)}$$

where C_0^r denotes a circle with radius r centered at the origin in the complex plane. Applying this, we can evaluate the sums and we now have

$$\langle|\mathscr{E}_L^*|^2\rangle_{\hat{\mathbf{r}}_1,\hat{\mathbf{r}}_2,\hat{\mathbf{R}}}=\frac{1}{r_1r_2R^2\pi i}\int_{C_0^1}dt\,\frac{1}{t(t+2)}$$

$$\times\int_0^{r_1}dx_1\left(\frac{2x_1}{R(t+2)}\right)^{2(L+1)}\frac{1}{1-(2x_1/R(t+2))^2}$$

$$\times\int_0^{r_2}dx_2\left(\frac{2x_2}{Rt}\right)^{2(L+1)}\frac{1}{1-(2x_2/Rt)^2} \qquad \text{(B10)}$$

We now get

$$\frac{1}{r}\int_0^r\frac{(ax)^j}{1-(ax)^2}\,dx$$

$$=\frac{1}{j+1}\frac{(ar)^j}{1-(ar)^2}\left\{1-[1-(ar)^2]\sum_{k=0}^{\infty}\frac{2k(ar)^{2k}}{j+2k+1}\right\}$$

By noticing that

$$[1-(ar)^2]\sum_{k=0}^{\infty}\frac{2k(ar)^{2k}}{j+2k+1}<\frac{1-(ar)^2}{j+1}\sum_{k=0}^{\infty}2k(ar)^{2k}$$

$$=\frac{1}{j+1}\frac{2(ar)^2}{1-(ar)^2}$$

we can write

$$\frac{1}{r}\int_0^r\frac{(ax)^j}{1-(ax)^2}\,dx=\frac{1}{j+1}\frac{(ar)^j}{1-(ar)^2}\left[1+O\left(\frac{1}{j+1}\right)\right] \qquad \text{(B11)}$$

Using the above, we get

$$\langle |\mathcal{G}_L^*|^2 \rangle_{\hat{r}_1, \hat{r}_2, \hat{R}} = \frac{1}{R^2 \pi i (2(L+1)+1)^2} \left(\frac{4 r_1 r_2}{R^2} \right)^{2(L+1)} \times \int_{C_0^1} \left(\frac{1}{t(t+2)} \right)^{2(L+1)+1} \times \frac{1}{1-(2r_1/R(t+2))^2} \frac{1}{1-(2r_2/Rt)^2} dt \tag{B12}$$

Consider the integral

$$\frac{1}{i} \int_{C_0^1} \left(\frac{1}{t(t+2)} \right)^j f(t)\, dt \tag{B13}$$

where $j \gg 1$, j odd, and $f(t)$ is some function of t. We can approximate the integral by an asymptotic expansion:

$$\frac{1}{i} \int_{C_0^1} \left(\frac{1}{t(t+2)} \right)^j f(t)\, dt = f(-1) \left(\frac{\pi}{j} \right)^{1/2} \left[1 + O\left(\frac{1}{j} \right) \right] \tag{B14}$$

Applying this, we get

$$\langle |\mathcal{G}_L^*|^2 \rangle_{\hat{r}_1, \hat{r}_2, \hat{R}} \approx \frac{1}{R^2 \sqrt{\pi}\, [2(L+1)+1]^{5/2}} \left(\frac{4 r_1 r_2}{R^2} \right)^{2(L+1)} \times \frac{1}{1-(2r_1/R)^2} \frac{1}{1-(2r_2/R)^2} \tag{B15}$$

Only the minimum values of R ($R=2$) are of importance, and we then get a term

$$(r_1)^{2(L+1)} \frac{1}{1-(r_1)^2} = (r_1)^{2(L+1)} \sum_{j=0}^{\infty} (r_1)^{2j} = \sum_{j=L+1}^{\infty} (r_1)^{2j} \tag{B16}$$

We find the expectation value using (B4),

$$\left\langle \sum_{j=L+1}^{\infty} (r_1)^{2j} \right\rangle_{r_1} = \frac{27}{8(L+1)(L+3/2)(L+2)} \left(\frac{\sqrt{3}}{2} \right)^{2(L+1)} \times \sum_{j=L+1}^{\infty} \frac{(L+1)(L+3/2)(L+2)}{j(j+1/2)(j+1)} \left(\frac{\sqrt{3}}{2} \right)^{2(j-L-1)} \tag{B17}$$

Now we can write the overall expectation value for $|\mathscr{E}_L^*|^2$, where we have multiplied by 6 because there are 6 cases having $R=2$:

$$\langle|\mathscr{E}_L^*|^2\rangle = \frac{6}{4\sqrt{\pi}\,[2(L+1)+1]^{5/2}}\left(\frac{27}{8(L+1)(L+3/2)(L+2)}\right)^2\left(\frac{3}{4}\right)^{2(L+1)} \times\left[\sum_{j=L+1}^{\infty}\frac{(L+1)(L+3/2)(L+2)}{j(j+1/2)(j+1)}\left(\frac{\sqrt{3}}{2}\right)^{2(j-L-1)}\right]^2 \tag{B18}$$

Observing that

$$\left[\sum_{j=L+1}^{\infty}\frac{(L+1)(L+3/2)(L+2)}{j(j+1/2)(j+1)}\left(\frac{\sqrt{3}}{2}\right)^{2(j-L-1)}\right]^2 < 7 \qquad \text{for} \quad 3\leqslant L\leqslant 10 \tag{B19}$$

we finally get

$$\langle|\mathscr{E}_L^*|^2\rangle = \frac{15309}{128\sqrt{\pi}\,[2(L+1)+1]^{5/2}(L+1)^2(L+3/2)^2(L+2)^2}\left(\frac{3}{4}\right)^{2(L+1)} \tag{B20}$$

Consider now the ratio

$$r \equiv \frac{\langle|\mathscr{E}_L^*|^2\rangle}{\langle\delta_L(\mathbf{s},\mathbf{r})^2\rangle} = \frac{63(L+1)(L+1/2)}{4\pi^{3/2}[2(L+1)+1]^{5/2}(L+3/2)(L+2)}\left(\frac{3\sqrt{3}}{4}\right)^{2(L+1)} \tag{B21}$$

Observing that $r<0.3$ for $L\leqslant 10$, we have shown that the $\mathscr{E}_L^*$ contribution is negligible compared to the corresponding δ_L contribution. Here it is very important to notice that this only applies for $L\leqslant 10$, as the $\mathscr{E}_L^*$ contribution becomes significantly bigger than the two other contributions for very large L ($r=12.6$ for $L=20$).

ACKNOWLEDGMENT

We gratefully acknowledge support from the Danish Research Council's special program in Information Technology.

REFERENCES

1. *QUANTA Parameter Handbook*, Polygen Corporation (1990).
2. M. P. Allen and D J. Tildesley, *Computer Simulations of Liquids* (Clarendon Press, Oxford, 1987).
3. T. Darden, D. York, and L. Pedersen, Particle mesh Ewald: An $n\log(n)$ method for Ewald sums in large systems, *J. Chem. Phys.* **98**:10089–10092 (1993).
4. S. W. de Leeuw, J. W. Perram, and E. R. Smith, Simulation of electrostatic systems in periodic boundary conditions. I. Lattice sums and dielectric constants, *Proc. R. Soc. Lond. A* **373**:27–56 (1980).
5. K. Esselink, Large-scale simulations of many-particle systems, Ph.D. thesis, Rijksuniversiteit Groningen, The Netherlands (1995).
6. I. S. Gradshteyn and I. M. Ryzhik, *Table of Integrals, Series and Products*, 5th ed. (Academic Press, New York, 1994).
7. L. Greengard and V. Rokhlin, A fast algorithm for particle simulations, *J. Comp. Phys.* **73**:325–348 (1987).
8. L. Greengard, The rapid evaluation of potential fields in particle systems, Ph.D. thesis, Yale University, New Haven, Connecticut (1987).
9. F. Leathrum, Jr., Parallelization of the fast multipole algorithm: algorithm and architecture design, Ph.D. thesis, Duke University, Durham, North Carolina, (1992).
10. J. Kolafa and J. W. Perram, Cutoff errors in the Ewald summation formulae for point charge systems, *Mol. Simul.* **9**:351–368 (1992).
11. H. G. Petersen, D. Sølvason, J. W. Perram, and E. R. Smith, The very fast multipole method, *J. Chem. Phys.* **101(10)**:8870 (1994).
12. H. G. Petersen, Accuracy and efficiency of the particle mesh Ewald method, *J. Chem. Phys.* **103(9)**:3668–3679 (1995).
13. H. G. Petersen, E. R. Smith, and D. Sølvason, Error estimates for the fast multipole method. II. The three-dimensional case, *Proc. R. Soc. Lond. A* **448**:401–418 (1995).